 https://doi.org/10.3311/PPci.40453

Periodica Polytechnica Civil Engineering, 69(3), pp. 904–914, 2025

Simple Model of Soil-structure Interaction in Horizontal Motion Taking into Account the Nonlinearity of the Soil

Yaseen Shayah[1*], László P. Kollár[1]

[1] Department of Structural Engineering, Faculty of Civil Engineering, Budapest University of Technology and Economics, Műegyetem rkp. 3., H-1111 Budapest, Hungary
[*] Corresponding author, e-mail: yaseen.shayah@edu.bme.hu

Received: 15 March 2025, Accepted: 30 May 2025, Published online: 13 June 2025

Abstract

Soil structure interaction is often modeled by lumped parameter models, which consist of connected springs, masses, and dashpots. It was shown that this model – even for the case of elastic behavior – can be rather inaccurate since radiation damping is not properly represented. Pap and her coauthor suggested a simple model that overcomes this problem: a simple infinitely long bar on an elastic foundation connected parallelly to a mass-spring system. Since soil nonlinearity can affect the response considerably, even in the case of moderate seismicity, Pap's model is extended in this paper for nonlinear soil behavior. As a result, the 3D nonlinear soil can be replaced by a simple beam resting on a foundation and connected parallelly to a mass-spring system. In addition to the three elastic properties, the level of plastification must be prescribed. This model is recommended for the practical modeling of soil-structure interaction when the nonlinearity of the soil is significant.

Keywords

soil-structure interaction, SSI, seismic analysis, radiation damping, linear, nonlinear

1 Introduction

Structures subjected to horizontal loads and wind are often analyzed by assuming a rigid connection to the ground. This approximation is unacceptable in the case of earthquakes, where the interaction between the structure and the soil affects the response significantly [1, 2]. The most accurate soil-structure interaction (SSI) analysis method is the direct method (Fig. 1(a)), where the soil and the structure are modeled together. This procedure can be very time-consuming and requires significant computational efforts.

For linear systems, the soil can be represented by the impedance functions, where the weightless foundation is subjected to a harmonic force, and the steady state response is given as the function of the exciting frequency [3]. In theory, for horizontal motions, the impedance functions (and hence the soil) can be represented by a spring and a dashpot, the characteristics of which depend on the frequency (Fig. 1(b)). Although these models can be analyzed, e.g., by the Fourier transform [3–5], it is rarely used in practical design.

A possible simplification is to use lumped parameter models (Figs. 1(c) and 1(e)). The simplest case is when one traditional spring and a dashpot are applied, where the characteristics are independent of the frequency (Fig. 1(c)) [6, 7]. When the vertical dimension of the soil is finite, this model can be unacceptably inaccurate [8–10]. The model can be refined by applying several springs and dashpots connected parallelly and serially (Fig. 1(e)), where the characteristics can be determined e.g., by the least square method [6, 11, 12]. The more complex model is applied, the more accurate solution can be achieved.

Pap and her coauthor argued [10] that these models are inefficient since radiation damping cannot be modeled with simple dashpot elements (Radiation damping occurs when the vibrating structure generates stress waves that radiate into an infinite or very large medium, for example, into the soil.). This is illustrated in Figs. 2 and 3 [13]. In Fig. 2, the impedance curves of a mass-spring system and an infinite bar on an elastic foundation are compared without damping. In the first case, there is no energy dissipation. In contrast, in the latter case, there is energy dissipation when the exciting frequency is above the cut-off (resonant) frequency (which is indicated by the ninety-degree phase shift). In Fig. 3, the two models with 5% damping ratio are compared; the significant difference between the two models is clearly visible. The infinite bar on an

Cite this article as: Shayah, Y., Kollár, L. P. "Simple Model of Soil-structure Interaction in Horizontal Motion Taking into Account the Nonlinearity of the Soil", Periodica Polytechnica Civil Engineering, 69(3), pp. 904–914, 2025. https://doi.org/10.3311/PPci.40453

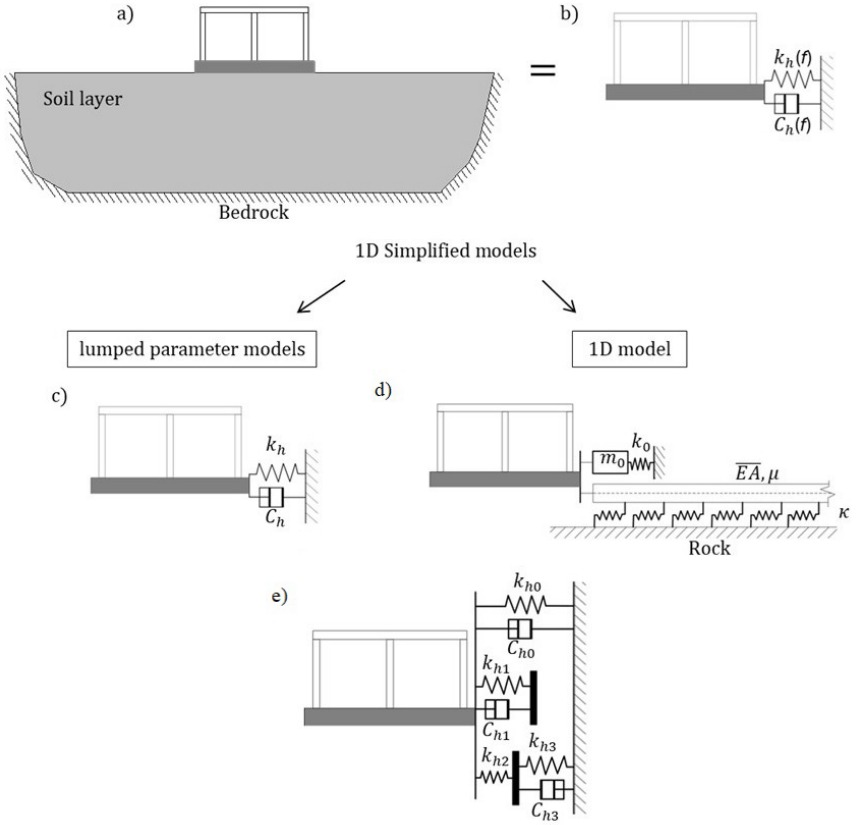

Fig. 1 a) Direct method, b) impedance function, c) lumped parameter model with one frequency independent spring and dashpot element, d) 1D model, e) complex lumped models

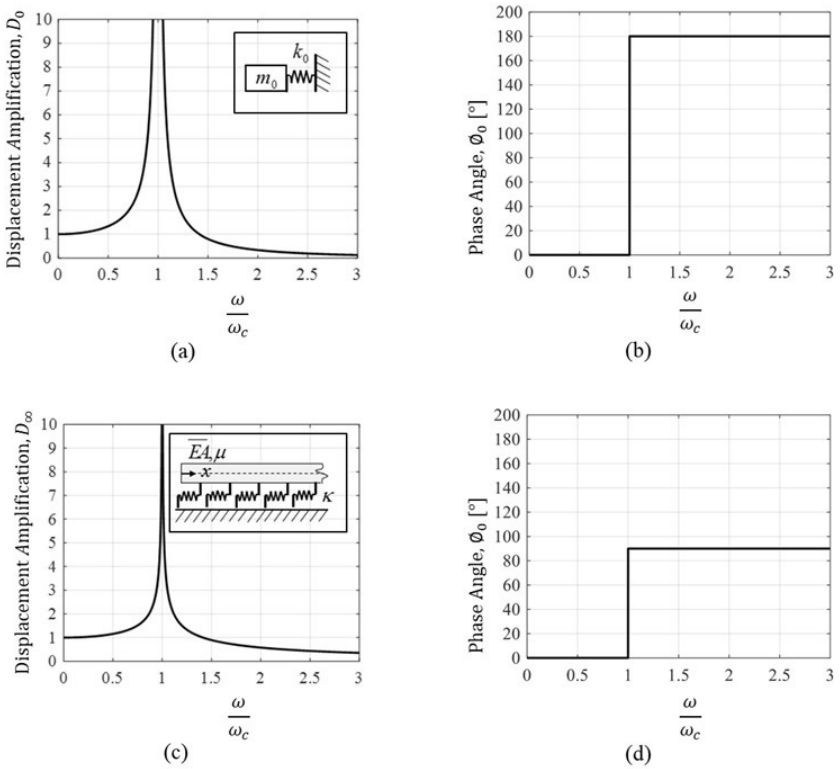

Fig. 2 (a) Impedance curves of a spring-mass system, (b) phase angle of a spring-mass system, (c) impedance curve of an axially constrained bar, (d) phase angle of an axially constrained bar (no damping) [13]

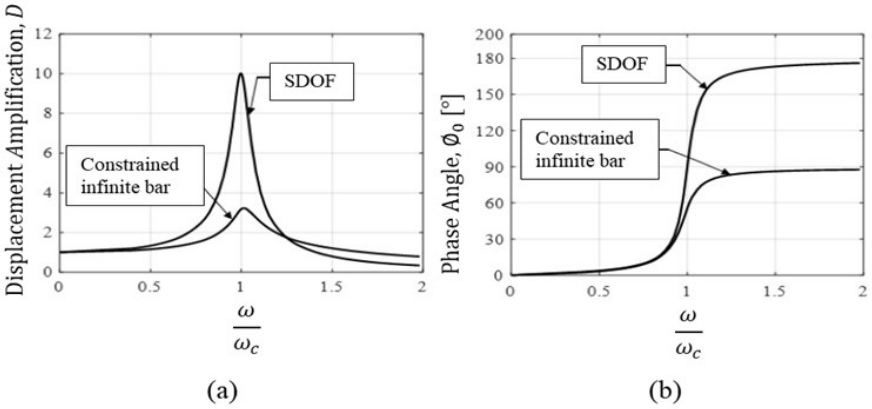

Fig. 3 (a) Amplification factor and (b) phase angle of the SDOF system and axially constrained infinite bar with damping ξ = 5% [13]

elastic foundation captures fairly well the radiation damping, which is important in modelling the soil.

Following a detailed investigation and validation, Pap suggested to apply a simple model for the soil (Fig. 1(d)): an infinitely long bar on an elastic foundation connected parallelly to a mass-spring system. This model has only three independent parameters: these are the resonant (cut-off) frequency (ω_c), the static stiffness (K), and the ratio (η), which shows the contribution of the two sub models: the infinite bar on an elastic foundation and the mass spring system. In addition, the damping coefficient (ξ), can be prescribed.

In [14], simple expressions were given for calculating these parameters for simple, regular cases, while an identification process was provided for complex, irregular cases. The expressions – for an infinitely long, uniform-height soil layer – are summarized in Fig. 4. In this figure, the characteristics of the model are defined: κ is the stiffness of the elastic foundation, $\overline{EA}$ is the tensile stiffness of the infinite bar, μ is mass per unit length, m_o is the equivalent mass and k_o is the spring constant. The relationships between the above three parameters (ω_c, K, η) and the characteristics of the sub-models are as follows [10]:

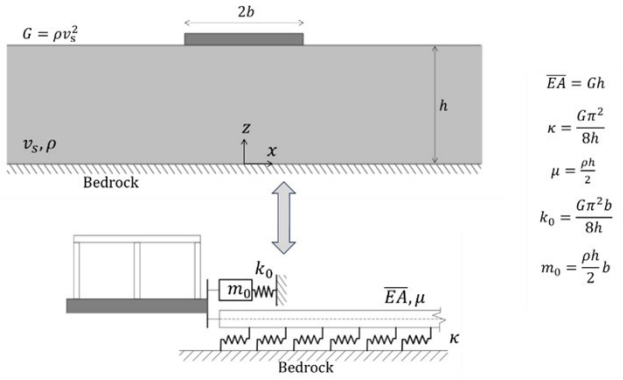

Fig. 4 Horizontally infinite soil layer with uniform thickness and the 1D equivalent model parameters

$$\eta = \frac{k_s}{K}, \quad \omega_c = \sqrt{\frac{\kappa}{\mu}} = \sqrt{\frac{k_o}{m_o}}, \quad K = k_s + k_o, \tag{1}$$

where

$$k_s = \sqrt{\kappa \overline{EA}} \tag{2}$$

Note that k_s is the static stiffness of the infinite bar on an elastic foundation [14], i.e., the force applied at the end of the bar, which results in unit end displacement. When the width of the foundation is significantly smaller than the height of the soil layer $\eta \approx 1$ and k_o, m_o are negligible.

The shortcomings of Pap's model are as follows:

- it was verified only for rigid structures (e.g. buildings); nevertheless, it was recommended to be used for MDOF structures as well.
- It can be applied only to linear models, i.e., for small strains in the soil.
- Although preliminary calculations show that a similar model should be applied for rocking, it was investigated in detail only for horizontal vibration.

For very small strains, the stress-strain relationship of the soil is given by Hooke's law: $\tau = G\gamma$, where τ is the shear stress, γ is the shear (angular) strain, while G is the constant shear modulus. The relationship between γ and τ is nonlinear for moderate shear strains, i.e., the shear modulus varies with the strain, as shown in (Fig. 5(a)) [15]. Note that soil undergoes plastic deformations when the strains are not very small. For unloading, hysteretic behavior occurs, which results in energy dissipation, as shown in (Fig. 5(b)). In [16, 17], we investigated under which circumstances (soil type, soil geometry, seismicity) the nonlinearity of the soil may play a role. It was found that even in the case of moderate seismicity, the nonlinearity should not be neglected.

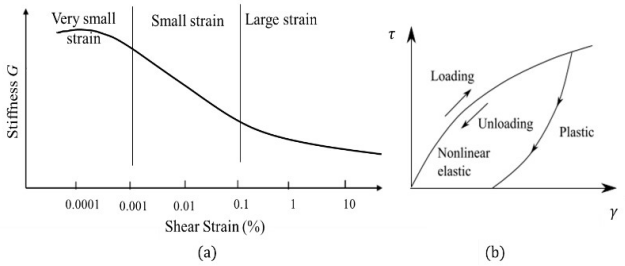

Fig. 5 (a) Stiffness-strain behavior of soil with typical strain ranges, and (b) nonlinear elastic and plastic model with hysteresis behavior [15]

It is worth noting that the method called Beam-on Nonlinear Winkler Foundation (BNWF) is an approach for modeling shallow foundations with nonlinear soil behavior, and the application of dashpots at the boundary of the FE mesh may also model energy dissipation. However, these models do not contain the fundamental behavior of soil, where radiation damping may play a role, and energy dissipation occurs only above the cut-off frequency, as discussed above [18].

2 Problem statement

It was stated in the Introduction that for horizontal excitation of linear SSI, Pap's model of an infinite bar on an elastic foundation should be used since the lumped parameter models cannot properly capture the radiation damping. This model should be

- generalized for nonlinear soil behavior (material nonlinearity) and
- the validation must include flexible structures.

Let us consider a flexible structure that is connected through a rigid foundation to the soil (Fig. 6). The bedrock surrounds the soil. The soil behaves in a linearly elastic manner when the angular strains are small; however, it has a hysteretic behavior at a given angular strain (Fig. 7). The bedrock is excited by horizontal earthquakes characterized

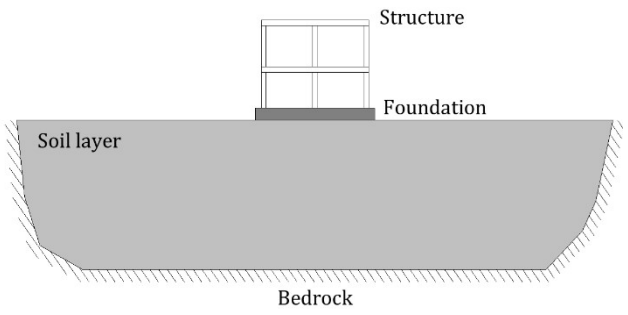

Fig. 6 Flexible structure connected to a rigid foundation and soil layer

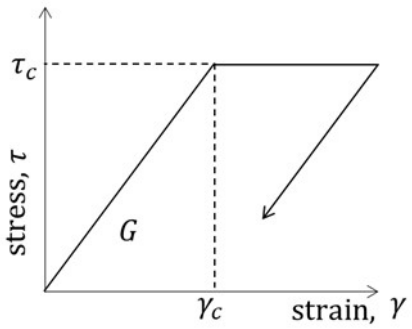

Fig. 7 2D Nonlinear material model

by their histograms. Here, we focus on buildings, where the slenderness of the building is small. Thus, the dominant motion of the structure is horizontal, i.e., rocking has a small effect only. The building behaves elastically. We aim to generalize Pap's model according to the two bullets listed above.

We have to admit the limitations of our aims. First, the nonlinearity is a complex phenomenon (Fig. 5), here we will focus only on an elastic perfectly plastic nonlinearity with full hysteresis. Second, our investigation is limited only to dominantly horizontal vibration, not rocking. Our aim is to demonstrate that Pap's model can be extended simply for cases with significant nonlinear behavior.

3 Approach, hypotheses

Pap's model has two sub-models (Fig. 1(d)) with the following characteristics:

- The infinite bar on an elastic foundation, with $\boldsymbol{\mu}$, $\boldsymbol{\kappa}$, $\overline{\boldsymbol{EA}}$
- The mass-spring model: $\boldsymbol{k_o}$ and $\boldsymbol{m_o}$

Note that the response of the system depends on three parameters only, listed in Eq. (1). It is assumed that the nonlinearity of the soil (Fig. 7) can be taken into account in Pap's model in such a way that the role of the elastic characteristics $\boldsymbol{\kappa}$, $\overline{\boldsymbol{EA}}$ (Eq. (1)) is changed: the model behaves in an elastic-plastic manner, with a hysteretic response, and it will be limited by ($\tau_{\overline{EA}}$ and $\boldsymbol{\tau_\kappa}$) or $\boldsymbol{N_0}$ and

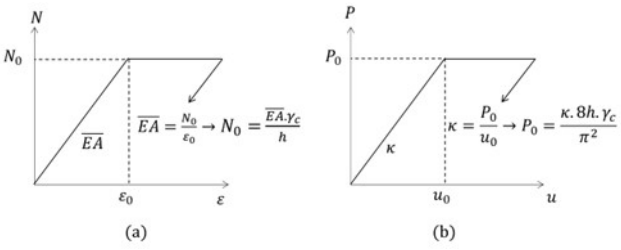

Fig. 8 Stiffness characteristics of 1D model of (a) the bar, and (b) the foundation

P_0 respectively as shown in (Fig. 8). These parameters were chosen in such a way that the linear calculation of the 2D (or 3D) model was compared to the 1D one, and the elastic limits were matched at identical displacements.

This model will be validated in this article by changing the following parameters:

- earthquake record (see, Table 1) [19, 20]
- soil geometry
- soil properties
- building geometry (rigid, one-, two-story, and seven story buildings) and mass
- level of plastification.

Most of our analyses are 2D (as it is very common in the literature [7, 10, 21] to prove the concept of lumped parameter models); however, to validate our model, also a 3D analysis is presented.

(We also investigated the possibility of limiting only one of the two elastic parameters (κ, $\overline{EA}$), but, as expected, both parameters had to be limited to get a good match with the 2D or 3D models.)

In the analysis, the damping ratio $\xi = 5\%$ is applied.

The response of the 2D (or 3D) model will be compared to that of the modified Pap's (1D) model, namely:

- the displacement (relative to the bedrock) function at the base, and their maximum values
- inter-story drifts of the building.

3.1 Finite Element Model

The 2D model was studied in ANSYS Mechanical APDL 2020 and Plaxis 2D (version 20.04.00790) by applying constraints on the vertical displacements. In the analysis, G was defined, and Poisson's ratio is $\nu = 0.3$. The height gives the model's geometry (soil) in the vertical direction, represented by h, and the length, l in the horizontal, x-direction.

For the "infinite" dimension, the length is selected to be sufficiently large so that the solution is not affected by changes in the length [10]. The earthquake excitation has been applied at the bedrock. Note that infinite bars cannot be modeled by finite length bars for elastic systems without damping because of the reflections from the boundary. However, when damping is present, a long, finite bar can capture the behavior of infinite bars well, as demonstrated by Pap.

Table 1 Earthquake records used in the analyses [19, 20]

ID	Earthquake Name	PGA [m/s^2]	Timestep Δt [s]	Length [s]
1	rec6	0.26	0.01	46
2	rec7	0.337	0.01	45.31
3	rec27	0.38	0.005	39.39
4	rec29	3.368	0.02	90.6
5	rec32	0.258	0.01	80
6	rec32.1	0.387	0.0025	20
7	RSN1050	2.26	0.02	19.98
8	rec32.3	4.45	0.01	22.3

For nonlinear analysis, the linear elastic perfectly plastic model has been employed. The soil is simulated using Ansys's bilinear kinematic hardening model [15] and the Mohr-Coulomb criterion in Plaxis [21]. Within the linear elastic perfectly plastic model, the initial slope of the curve corresponds to the material's elastic modulus. Plastic strain occurs when the stress surpasses a specified yield threshold.

In the 2D model, the Plane183 element, a higher-order 2D element with eight nodes, was used in the modeling. This element has two degrees of freedom at each node: displacement in the x and y directions [22]. For the 1D case, the bar is represented by BEAM188 elements, linear springs are simulated using COMBIN14 elements, nonlinear springs with COMBIN39 elements, and masses are modeled using MASS21 elements. In a few cases, Plaxis 2D was utilized to compare Ansys's results, which showed a reasonable match.

3.2 Mesh sensitivity

The mesh size should be less than one-eighth of the wavelength related to the maximum frequency component $f_{\max}$ of the input wave [23, 24], which is a widely used approach in dynamic modeling to assure consistent results. The recommended mesh size is:

$$\frac{L}{8} = \frac{Tv}{8} = \frac{v}{8f_{\max}} \tag{3}$$

The frequency spectrum of common earthquakes falls within the 0.45 Hz to 2.82 Hz range, determined through an analysis of 44 far-field records from FEMA [10]. Substituting the minimum velocity of 100 m/s and the maximum frequency $f = 2.82$ Hz gives an average element size of 4.43 m. However, all models employ a mesh size ranging from 1 m to 2 m, which is significantly smaller than 4.43 m.

4 Validation

First, an infinitely long 50 m height soil layer (Fig. 4) was investigated and subjected to eight earthquake records listed in Table 1. The infinitely long dimension of the layer was replaced in the FE analysis by 1000 m. The results are shown in Tables 2–5. In the four cases, the width of the foundation ($2b$) and the soil stiffness (i.e., the shear wave

Table 2 Maximum responses of the 2D and 1D models subjected to earthquakes, $2b$ = 20 m, v_s = 100 m/s

Case		τ_{max}			τ_c = 100 kN/m²		τ_c = 75 kN/m²	
Record	τ_{max} kN/m²	$u_{\frac{\max}{2D}}$	$u_{\frac{\max}{1D}}$	$\frac{u_{\frac{\max}{1D}}}{u_{\frac{\max}{2D}}}$	$\frac{u_{\frac{\max(\tau=100)}{2D}}}{u_{\frac{\max}{2D}}}$	$\frac{u_{\frac{\max(\tau=100)}{1D}}}{u_{\frac{\max}{1D}}}$	$\frac{u_{\frac{\max(\tau=75)}{2D}}}{u_{\frac{\max}{2D}}}$	$\frac{u_{\frac{\max(\tau=75)}{1D}}}{u_{\frac{\max}{1D}}}$
rec6	125	0.033	0.032	97%	81%	78%	71%	69%
rec7	136	0.037	0.034	92%	79%	77%	66%	70%
rec27	147	0.053	0.052	97%	67%	74%	67%	65%
rec29	185	0.128	0.115	90%	80%	82%	71%	73%
rec32	133	0.091	0.088	96%	85%	88%	66%	65%
rec32.1	115	0.019	0.015	83%	80%	83%	66%	70%

Table 3 Maximum responses of the 2D and 1D models subjected to earthquakes, $2b$ = 40 m, v_s =100 m/s

Case		τ_{max}			τ_c = 100 kN/m²		τ_c = 75 kN/m²	
Record	τ_{max} kN/m²	$u_{\frac{\max}{2D}}$	$u_{\frac{\max}{1D}}$	$\frac{u_{\frac{\max}{1D}}}{u_{\frac{\max}{2D}}}$	$\frac{u_{\frac{\max(\tau=100)}{2D}}}{u_{\frac{\max}{2D}}}$	$\frac{u_{\frac{\max(\tau=100)}{1D}}}{u_{\frac{\max}{1D}}}$	$\frac{u_{\frac{\max(\tau=75)}{2D}}}{u_{\frac{\max}{2D}}}$	$\frac{u_{\frac{\max(\tau=75)}{1D}}}{u_{\frac{\max}{1D}}}$
rec6	113	0.031	0.027	86%	83%	82%	66%	68%
rec7	122	0.034	0.030	88%	82%	83%	68%	69%
rec27	132	0.050	0.045	90%	84%	86%	67%	70%
rec29	167	0.123	0.110	90%	78%	79%	61%	58%
rec32	120	0.091	0.081	89%	83%	84%	70%	69%

Table 4 Maximum responses of the 2D and 1D models subjected to earthquakes, $2b$ = 20 m, v_s = 200 m/s

Case		τ_{max}			τ_c = 100 kN/m²		τ_c = 75 kN/m²	
Record	τ_{max} kN/m²	$u_{\frac{\max}{2D}}$	$u_{\frac{\max}{1D}}$	$\frac{u_{\frac{\max}{1D}}}{u_{\frac{\max}{2D}}}$	$\frac{u_{\frac{\max(\tau=100)}{2D}}}{u_{\frac{\max}{2D}}}$	$\frac{u_{\frac{\max(\tau=100)}{1D}}}{u_{\frac{\max}{1D}}}$	$\frac{u_{\frac{\max(\tau=75)}{2D}}}{u_{\frac{\max}{2D}}}$	$\frac{u_{\frac{\max(\tau=75)}{1D}}}{u_{\frac{\max}{1D}}}$
rec6	139	0.036	0.031	87%	83%	86%	70%	74%
rec7	140	0.032	0.026	82%	82%	85%	76%	81%
rec27	140	0.035	0.031	88%	88%	88%	71%	74%
rec29	178	0.092	0.080	86%	84%	94%	73%	76%
rec32	191	0.097	0.090	93%	93%	91%	75%	74%

Table 5 Maximum responses of the 2D and 1D models subjected to earthquakes, $2b$ = 50 m, v_s = 250 m/s

Case		τ_{max}			τ_c = 100 kN/m²	
Record	τ_{max} kN/m²	$u_{\frac{\max}{2D}}$	$u_{\frac{\max}{1D}}$	$\frac{u_{\frac{\max}{1D}}}{u_{\frac{\max}{2D}}}$	$\frac{u_{\frac{\max(\tau=100)}{2D}}}{u_{\frac{\max}{2D}}}$	$\frac{u_{\frac{\max(\tau=100)}{1D}}}{u_{\frac{\max}{1D}}}$
rec6	175	0.028	0.027	97%	77%	76%
rec7	137	0.021	0.019	90%	80%	80%
rec27	186	0.029	0.027	94%	79%	82%
rec29	345	0.060	0.056	94%	70%	74%
rec32.1	172	0.027	0.026	98%	77%	76%

velocity v_s, $G = \rho v_s^2$) were varied, as listed in the table captions. An elastic analysis and two elastic-plastic analyses were considered: the plastic shear strains (τ_c, Fig. 7) of the soil were given as 100 and 75 kN/m^2, corresponding to about 80% and 60% of the maximum elastic shear stresses.

The characteristics of the 1D sub-models were calculated using the expressions given in Fig. 4. The results for the four cases are given in the first four rows of Table 6. For the nonlinear analysis $\boldsymbol{\kappa}$ and $\overline{\boldsymbol{EA}}$ are used only below 80% and 60% of the maximum elastic strains (see Fig. 8).

The maximum shear stress obtained from the elastic 2D FE analysis is given in the second column of Tables 2–5, while the maximum displacements (under the middle of the foundation) are in the 3rd column. The displacements calculated from the 1D model are given in the 4th column, while their ratios are presented in the 5th column. In almost all cases, the results of the accurate (2D) and approximate (1D) calculations are very close to each other. (Note that the accuracy of the accelerations is somewhat less good.)

In every case, the plasticity reduces the displacements; in the last 2 × 2 columns, the ratios of the plastic and elastic displacements are given; it is clearly shown that the decrease in the 1D model is very close to that of the "accurate" 2D model. The results of the time history analyses of the 2D and the 1D models are given as illustrative examples for one particular case in Fig. 9 (a and b).

Now, we investigate the case presented in Table 3; the only difference is that the layer has a finite length of l = 200 m (Fig. 10(a)). In this case, the simple expressions given in Fig. 4 are not applicable; instead, the procedure presented in [14] - based on the impedance curve – was applied.

The characteristics of the 1D model are given in the 5th row of Table 6. Comparisons of the 2D and 1D analyses are given in Table 7.

Next, the same model was considered, but the soil characteristic was changed as v_s = 250 m/s. The calculated characteristics of the 1D model are given in the 6th row of Table 6, the results are presented in the 3rd row of Table 7. It is observed that there is good agreement between the 2D and 1D solutions.

So far, the structure – following Pap's examples – was considered to be a rigid object. Now, our comparison is extended to flexible structures. First, a one and a two-story building with different story stiffness are considered (Figs. 10(b) and 10(c)). In the first case, the building can be characterized well by one degree of freedom, while two degrees of freedom in the second.

It is worthwhile to mention that when modeling the flexible structure (e.g., building), the building has been built as a real structure either in the 1D model (see Fig. 1(d)) or in the 2D model (see Figs. 10(b) and 10(c)). (However,

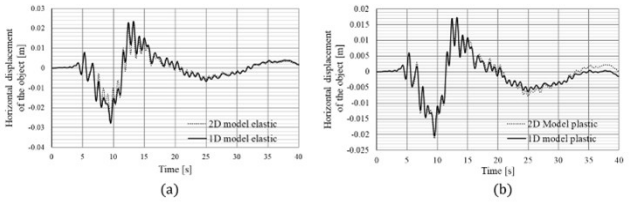

Fig. 9 Comparison of the time history analyses of the 2D and 1D model given in Table 5, 1st row, 2b = 50 m, v = 250 m/s, record 6, a) elastic analysis, b) plastic analysis (τ_c = 100)

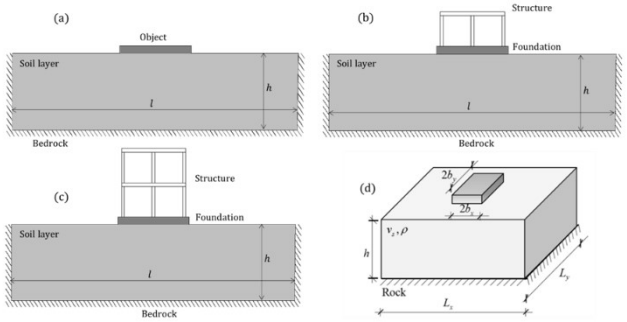

Fig. 10 Finite length soil layer, a) rigid structure, b) one story flexible structure and, c) two story structure, d) 3D model with a shallow foundation

Table 6 Characteristics of the elastic 1D models used in the validation

case	$k_o \times 10^6$ [N/m^2]	$\kappa \times 10^6$ [N/m^2]	$EA \times 10^6$ [N]	$\mu \times 10^3$ [kg/m]	$m_o \times 10^5$ [kg]	→	ω_c [1/s]	$K \times 10^6$ [N/m^2]	η
1 (Table 2)	-	4.44	900	45	-		3.14	20	1
2 (Table 3)	8.88	4.44	900	45	9		3.14	28.87	0.69
3 (Table 4)	-	1.77	3600	45	-		6.28	80	1
4 (Table 5)	69.39	2.77	5625	45	11.25		7.85	194.35	0.64
5 (Table 7-a)	-	-	-	-	-		3.68	38.1	0.65
6 (Table 7-b)	-	-	-	-	-		9.17	229	0.68
7 (Fig. 10, d)	61.6	4013	4200	336	51.6		3.46	4167	0.98
8 (Fig. 13)	14.9	27.44	27.5	1555	8.47		4.2	42.4	0.65

Table 7 Maximum responses of the 2D and 1D models subjected to earthquakes (Fig. 10(a)), l = 200 m: (a) $2b$ = 40 m, v_s = 100 m/s,(b) $2b$ = 40 m, v_s = 250 m/s

Case		τ_{max}		τ_c = 100 kN/m²			τ_c = 75 kN/m²	
Soil	Record	$\frac{u_{max}}{2D}$	$\frac{u_{max}}{1D}$	$\frac{u_{\frac{max}{1D}}}{u_{\frac{max}{2D}}}$	$\frac{u_{\frac{max(\tau=100)}{2D}}}{u_{\frac{max}{2D}}}$	$\frac{u_{\frac{max(\tau=100)}{1D}}}{u_{\frac{max}{1D}}}$	$\frac{u_{\frac{max(\tau=75)}{2D}}}{u_{\frac{max}{2D}}}$	$\frac{u_{\frac{max(\tau=75)}{1D}}}{u_{\frac{max}{1D}}}$
a	Rec6	0.023	0.024	106%	79%	78%	63%	60%
	Rec32.3	0.127	0.126	99%	77%	75%	64%	62%
b	Rec32.3	0.083	0.090	108%	84%	81%	63%	56%

a possible simplification is replacing the building with a one- or two-degree freedom system that includes springs and masses. We found practically no numerical difference between the MDF modeling of the building and the simplified modeling.)

The results are given for the one-story and two-story buildings in Tables 8 and 9. In all cases, the results of the accurate (2D) and approximate (1D) analyses are reasonably close to each other.

Fig. 11 illustrates the drift story u_{2-1} for the – nonlinear analysis - for the first case outlined in Table 8 and Fig. 10(b). The drift calculated using the simplified model and the direct approach results are plotted with solid and dashed lines, respectively. The comparison demonstrates that the present model offers a reasonably accurate approximation of the results obtained from the direct 2D analysis.

The method can be expanded in the following example to address 3D problems involving shallow foundations. The problem investigated by [10] and illustrated in Fig. 10(d) is analyzed. The problem presented involves an object subjected to earthquake record no. 32.3 (see Table 1). The following parameters have been used, h = 50 m, b_x = 20 m, b_y = 40 m, v_s = 100 m/s, L_x = 1400 m, L_y = 200 m. The 1D model parameters have been calculated using the procedure – based on the impedance curve – mentioned in [10]; these parameters are given in the 7th row of Table 6. The displacements are assessed and compared at the center of the foundation, specifically at the bottom center of the foundation, which corresponds to the top level of the soil layer. As illustrated in Fig. 12, the solid lines represent the horizontal displacements obtained from the direct approach, while the dashed line

Table 8 Maximum responses of the 2D and 1D models subjected to earthquakes, one-story structure, (Fig. 10(b)), $2b$ = 20 m, t_{wall} = 0.4 m, t_{slab} = 0.2 m, and h_{storey} = 3 m

Case		Linear			Storey drift	
		1st storey			Linear	Nonlinear τ = 100 kN/m²
Shear Velocity [m/s]	Record	u_{2D}	u_{1D}	u_{1D}/u_{2D}	$\frac{u_{1D}/u_{2D}}{u_{1-base}}$	$\frac{u_{1D}/u_{2D}}{u_{1-base}}$
200	rec32.3	0.110	0.119	93%	103%	105%
100	rec32.3	0.148	0.147	100%	102%	86%
100	rec29	0.576	0.502	115%	102%	117%

Table 9 Maximum responses of the 2D and 1D models subjected to earthquakes, two-story structure, (Fig. 10(c)), $2b$ = 20 m, t_{wall} = 0.4 m, t_{slab} = 0.2 m, and h_{storey} =3 m

Case		Linear						Storey drift			
		2nd storey			1st storey			Linear		Nonlinear τ = 100 kN/m²	
Shear Velocity [m/s]	Record	u_{2D}	u_{1D}	u_{1D}/u_{2D}	u_{2D}	u_{1D}	u_{1D}/u_{2D}	$\frac{u_{1D}/u_{2D}}{u_{2-1}}$	$\frac{u_{1D}/u_{2D}}{u_{1-base}}$	$\frac{u_{1D}/u_{2D}}{u_{2-1}}$	$\frac{u_{1D}/u_{2D}}{u_{1-base}}$
200	rec32.3	0.116	0.144	81%	0.113	0.134	84%	120%	86%	83%	91%
100	rec32.3	0.182	0.216	84%	0.180	0.172	105%	81%	103%	96%	111%
100	rec29	0.586	0.552	106%	0.584	0.518	113%	80%	99%	85%	82%

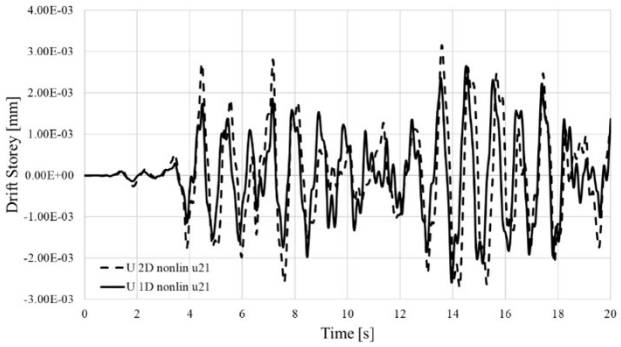

Fig. 11 Drift story u_{2-1} for the first case of Table 8, with v_s = 200 m/s, l = 200 m: 2b = 20 m

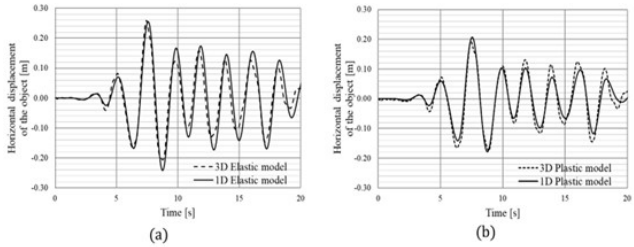

Fig. 12 Comparison of the time history analyses of the 3D (Fig. 10(d)) and 1D model given in (Table 6, 7th row), a) elastic analysis, b) plastic analysis (τ_c = 100)

corresponds to the results from the simplified model. This comparison visually highlights the relationship between the two methods and their outcomes. The comparison reveals that the current model reasonably approximates the outcomes from the direct 3D analysis.

Another 2D example is presented, Fig. 13, presenting a common structural system used in buildings, the shear wall system. The model consists of a seven-story building with a total height of h_{str} = 28 m, supported by a raft foundation (2b = 50 m wide and 1 m thick).

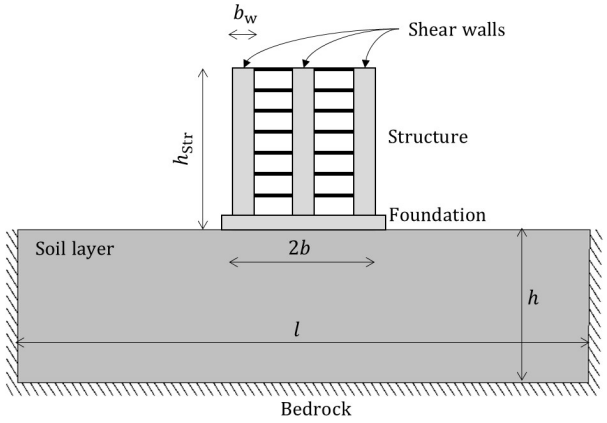

Fig. 13 Finite length soil layer with 7 storey building l = 200 m h = 50 m

Three shear walls (each has b_w = 5 m wide and 0.5 m thick) resist the horizontal seismic applied loads. The soil domain beneath the structure extends l = 200 m in width and h = 50 m in depth with shear wave velocity v_s = 100 m/s. The 1D model parameters were calculated using the impedance-based procedure described in [10], and the results are listed in the 8th row of Table 6.

Displacements are evaluated and compared at the center of the foundation base, aligning with the top surface of the soil layer. As shown in Fig. 14, solid lines depict horizontal displacements from the direct method, while the dashed line represents results from the simplified model. It demonstrates that the simplified model reasonably approximates the direct 2D analysis outcomes. Although the simplified method produces a smoother curve than the direct method, their maximum and minimum values are in close agreement. Furthermore, in the 2D plastic analysis, the maximum top displacement relative to the bottom is 0.199 m, while the maximum displacement of the foundation is 0.11 m. For comparison, the corresponding values obtained from the 1D model are 0.203 m and 0.112 m, respectively, indicating good agreement with the 2D result.

Another comparative analysis was also conducted for four story structure (Fig. 13). The results show good agreement between the curves predicted by the simplified model (solid line) and those obtained from the FEM analysis (dashed line). See Fig. 15.

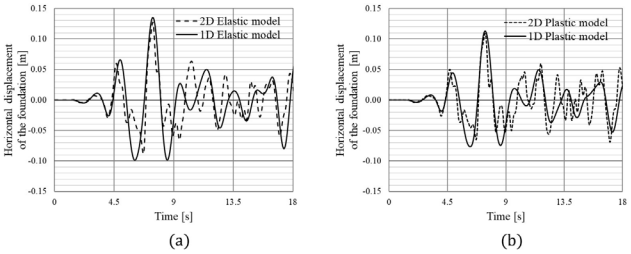

Fig. 14 Comparison of the time history analyses of the 2D (Fig. 13) and 1D model given in (Table 6, 8th row), a) elastic analysis, b) plastic analysis (τ_c = 100)

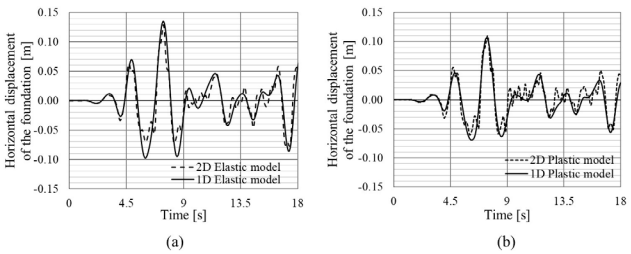

Fig. 15 Comparison of the time history analyses of the 2D (4 story-building) and 1D model; a) elastic analysis, b) plastic analysis (τ_c = 100)

5 Discussion

In this paper Pap's model was extended for nonlinear soil behavior. Recall that even for elastic behavior the lumped mass models can be rather inaccurate, and Pap's simple model, which depends on three parameters only, are recommended to be applied. Since the soil nonlinearity can affect the response considerably even in the case of moderate seismicity, our findings that Pap's model can be simply extended for nonlinear behavior is an important result. As a consequence, the 3D (or 2D) nonlinear soil can be replaced by a simple infinitely long beam resting on a foundation and connected parallelly to a mass-spring system. In addition to the three elastic properties the level of plastification must be prescribed.

We consider that our main finding is *the extremely small number of parameters* needed to prescribe the response to a rather complex task. It could be reached due to the fact that Pap's model can capture the fundamental behavior of the soil. (The problem was solved by a very long bar resting on an elastic-plastic foundation; however, in the future, we plan to explore other – hopefully more efficient – solution techniques). The results were validated by several numerical examples, where the soil parameters, geometry, seismicity and the characteristics of the buildings were varied.

Although for the practical applications in more general cases further research is needed, the enhanced Pap's model seems applicable to model the soil even in the case of significant plastification. To further extend its applicability and accuracy, future work should focus on several key aspects. These include the application of flexible foundation conditions and the influence of stiffness contrast between the superstructure and the soil, the incorporation of additional kinematic fields to better represent the behavior of flexible soils, and the evaluation of P-Delta effects. Furthermore, the inclusion of rocking mechanisms within the model framework.

Acknowledgement

The Stipendium Hungaricum Scholarship provided by the Tempus Public Foundation to Yaseen Shayah is highly appreciated.

References

[1] Kramer, S. "Geotechnical Earthquake Engineering", Pearson Education India, 1996. ISBN: 978-0133749434

[2] Wilson, E. L. "Three-dimensional static and dynamic analysis of structures", Computers and Structures, Inc., 1996. ISBN: 0-923907-00-9

[3] Kausel, E. "Early history of soil–structure interaction", Soil Dynamics and Earthquake Engineering, 30(9), pp. 822–832, 2010. https://doi.org/10.1016/j.soildyn.2009.11.001

[4] Hayashi, Y., Katukura, H. "Effective time-domain soil-structure interaction analysis based on FFT algorithm with causality condition", Earthquake Engineering & Structural Dynamics, 19(5), pp. 693–708, 1990. https://doi.org/10.1002/eqe.4290190506

[5] Nakamura, N. "Basic Study on the Transform Method of Frequency-Dependent Functions into Time Domain: Relation to Duhamel's Integral and Time-Domain-Transfer Function", Journal of Engineering Mechanics, 138(3), pp. 276–285, 2012. https://doi.org/10.1061/(ASCE)EM.1943-7889.0000330

[6] Wolf, J. P. "Foundation Vibration Analysis Using Simple Physical Models", Pearson Education, 1994. ISBN: 9780132442022

[7] Lysmer, J., Richart Jr, F. E. "Dynamic Response of Footings to Vertical Loading", Journal of the Soil Mechanics and Foundations Division, 92(1), pp. 65–91, 1966. https://doi.org/10.1061/JSFEAQ.0000846

[8] Mylonakis, G., Nikolaou, S., Gazetas, G. "Footings under seismic loading: Analysis and design issues with emphasis on bridge foundations", Soil Dynamics and Earthquake Engineering, 26(9), pp. 824–853, 2006. https://doi.org/10.1016/j.soildyn.2005.12.005

[9] Dunn, P. W. "Comparison of cone model and measured dynamic impedance functions of shallow foundations", PhD Thesis, University of Florida, 2010.

[10] Pap, Z. B. "The role of radiation damping in the dynamic response of structures", PhD Thesis, Budapest University of Technology and Economics, 2020. [online] Available at: http://hdl.handle.net/10890/13369 [Accessed: 10 March 2025]

[11] Wolf, J. P. "Spring-dashpot-mass models for foundation vibrations", Earthquake Engineering & Structural Dynamics, 26(9), pp. 931–949, 1997. https://doi.org/10.1002/(SICI)1096-9845(199709)26:9<931::AID-EQE686>3.0.CO;2-M

[12] Wolf, J. P. "Consistent lumped-parameter models for unbounded soil: Physical representation", Earthquake Engineering & Structural Dynamics, 20(1), pp. 11–32, 1991. https://doi.org/10.1002/eqe.4290200103

[13] Pap, Z. B., Kollar, L. P. "The dynamic response of infinitely long constrained bars and its application for modelling SSI", Structures, 34, pp. 875–885, 2021. https://doi.org/10.1016/j.istruc.2021.07.082

[14] Pap, Z. B., Kollár, L. P. "Model of Soil-structure Interaction of Objects Resting on Finite Depth Soil Layers for Seismic Design", Periodica Polytechnica Civil Engineering, 63(4), pp. 1204–1216, 2019. https://doi.org/10.3311/PPci.14459

[15] Arkinsos, J. H., Sallfors, G. "Experimental determination of soil properties", In: Proceedings of the 10th ECSMFE, Florence, Italy, 1991, pp. 915–956.

[16] Shayah, Y., Kollár, L. P. "Role of Nonlinearity in the Soil in Earthquake-Resistant Design of Structures", Periodica Polytechnica Civil Engineering, 67(3), pp. 914–924, 2023. https://doi.org/10.3311/PPci.21641

[17] Shayah, Y., Kollár, L. P. "Significance of Soil Nonlinearity in Soil Structure Interaction", In: fib Symposium, 15th fib International PhD Symposium in Civil Engineering, Budepst, Hungary, 2024, pp. 85–92. ISBN: 978-294064324-0

[18] Shayah, Y. "Soil structure interaction and the radiation damping: A state-of-the-art review", Results in Engineering, 26, 104755, 2025. https://doi.org/10.1016/j.rineng.2025.104755

[19] Applied Technology Council "Quantification of Building Seismic Performance Factors", Federal Emergency Management Agency, Washington, DC, USA, P. 695, 2009.

[20] PEER "PEER Ground Motion Database", [online] Available at: https://ngawest2.berkeley.edu/ [Accessed: 10 March 2025]

[21] Dobry, R., Gazetas, G. "Dynamic Response of Arbitrarily Shaped Foundations", Journal of Geotechnical Engineering, 112(2), pp. 109–135, 1986. https://doi.org/10.1061/(ASCE)0733-9410(1986)112:2(109)

[22] ANSYS "ANSYS mechanical APDL material reference", ANSYS Inc, 2020.

[23] Lysmer, J., Kuhlemeyer, R. L. "Finite dynamic model for infinite media", Journal of the Engineering Mechanics Division, 95(4), pp. 859–877, 1969. https://doi.org/10.1061/JMCEA3.0001144

[24] Bathe, K.-J. "Finite element procedures", Klaus-Jurgen Bathe, 2007. ISBN: 978-0979004902